CDK9 and its repressor LARP7 modulate cardiomyocyte proliferation and response to injury in the zebrafish heart

Title: CDK9 and its repressor LARP7 modulate cardiomyocyte proliferation and response to injury in the zebrafish heart

Authors: Gianfranco Matrone PhD [1,2], Kathryn S. Wilson PhD[1], Sana Maqsood BSc[1], John J. Mullins PhD[1], Carl S. Tucker PhD[1], Martin A. Denvir MD, PhD[1]*

Affiliations:

1. British Heart Foundation Centre for Cardiovascular Science, The Queen's Medical Research Institute, The University of Edinburgh, Edinburgh, EH16 4TJ, United Kingdom

2. Center for Cardiovascular Regeneration, Department of Cardiovascular Sciences, Methodist Hospital Research Institute, Houston 77030, Texas

Author for correspondence: *Dr Martin Denvir, BHF Centre for Cardiovascular Science, The Queen's Medical Research Institute, The University of Edinburgh, Edinburgh, EH16 4TJ.
Tel. 0044 131 242 9236, Email: mdenvir@staffmail.ed.ac.uk

Key words: zebrafish, CDK9, LARP7, heart, repair.

ABSTRACT

Cyclin Dependent Kinase (CDK)9 acts via the Positive Transcription Elongation Factor-b (P-TEFb) complex to activate and expand transcription via RNA polymerase II (RNApol II). It has also been shown to regulate cardiomyocyte hypertrophy with recent evidence linking it to cardiomyocyte proliferation. We hypothesised that modification of CDK9 activity could both impair and enhance the cardiac response to injury by modifying cardiomyocyte proliferation.

CDK9 expression and activity were inhibited in the zebrafish (*Danio rerio*) embryo. We show that dephosphorylation of the Serine2 residue on the Carboxy-Terminal domain of RNApol II (Ser2-RNApol II-CTD) is associated with impaired cardiac structure, function and cardiomyocyte proliferation and also results in impaired functional recovery following cardiac laser injury. In contrast, de-repression of CDK9 activity, by knockdown of La-related protein (LARP7) increases phosphorylation of Ser2-RNApol II-CTD and increases cardiomyocyte proliferation. LARP7 knockdown rescued the structural and functional phenotype associated with knockdown of CDK9.

CDK9/LARP7-balance plays a key role in cardiomyocyte proliferation and response to injury. LARP7 represents a potentially novel therapeutic target in promoting cardiomyocyte proliferation and recovery from injury.

INTRODUCTION

Cyclin Dependent Kinase 9 (CDK9) has emerged from the wider family of CDKs as an important signaling mechanism in the initiation and progression of cardiac hypertrophy (Krystof et al., 2012, Krystof et al., 2010). Sano and colleagues (Sano et al., 2002) showed that CDK9 expression is up-regulated and activity enhanced during cardiac hypertrophy and that chronic activation of CDK9 predisposes to heart failure in adult mouse myocardium. More recently, CDK9 has been shown to act as a binding partner of GATA4, an important regulator of cardiomyocyte proliferation in mammals and zebrafish (Kikuchi et al., 2010). This link to GATA4 provides support for a possible role of CDK9 in regulating cardiomyocyte proliferation (Sunagawa et al., 2010).

In mammalian species, cardiomyocytes proliferate rapidly during fetal life but lose this capacity within the weeks and months following birth leaving only a very low level of background mitosis in adult hearts (Ahuja et al., 2007). The zebrafish heart, on the other hand, retains a much higher rate of background cardiomyocyte cell division throughout adulthood associated with a remarkable capacity to regenerate cardiac tissue following injury (Poss et al., 2002). An additional contrasting feature of the zebrafish heart is that, unlike the mammalian heart, it appears to lack a classical hypertrophic response although few hypertrophic models have been developed in the fish (Sun et al., 2009). Indeed, Becker and colleagues (Becker et al., 2011) showed that a troponin T (tnnt2) gene knockdown targeting the exon 13 splice donor site in embryonic zebrafish, designed to mimic human hypertrophic cardiomyopathy, resulted in cardiomyocyte hyperplasia and a dilated ventricle despite a switch in expression to molecular pathways associated with hypertrophy.

Cardiac hypertrophy is typically associated with a global increase in mRNA and protein synthesis in cardiomyocytes. CDKs are a family of cell cycle regulators closely linked to transcription (Garriga and Grana, 2004, Loyer et al., 2005). Indeed, persistent endogenous CDK inhibition in adult cardiomyocytes has been proposed as one of the reasons why these cells rarely re-enter the cell cycle following injury or in response to haemodynamic or other stress. In support of this, knockdown of endogenous CDK inhibitors by small interfering RNA was found to induce neonatal and adult cardiomyocytes to re-enter the cell cycle resulting in active proliferation of previously quiescent cells (Di Stefano et al., 2011). This intriguing finding suggests a key role for CDKs in controlling the proliferative behaviour of cardiomyocytes and points to a potential mechanism by which cardiomyocytes could be induced to divide.

CDK9 becomes active by complexing with Cyclin T, forming the Positive Transcription Elongation Factor b (P-TEFb), leading to enhanced transcriptional activity via RNA polymerase II (RNApol II). Inactivation results from binding to hexamethylene bisacetamide-induced protein (HEXIM) 1 and/or HEXIM2 (Barboric et al., 2005, Yik et al., 2003) and the La-related protein 7 (LARP7) (He et al., 2008, Markert et al., 2008). La-related protein (LARP)7, also called PIP7S (He et al., 2008), is a highly specialized RNA-binding molecule which stabilizes the CDK9 inactivating complex by providing a bridge between 7SK-RNA and HEXIM. Indeed, a previous study (Markert et al., 2008) using silencing-RNA against LARP7 caused upregulation of RNA pol II activity. LARP7 therefore appears to be an important regulator of CDK9 and consequently of P-TEFb complex activity (Krueger et al., 2008).

These regulatory mechanisms provide novel and important insights into ways in which CDK9 could be manipulated for therapeutic benefits. Indeed, while pharmacological CDK9 inhibition has been proposed as a therapy for abrogating cardiac hypertrophy (Krystof et al., 2010) the possibility of enhancing CDK9 activity has been overlooked as a mechanism to induce cardiac hypertrophy and or stimulate cardiomyocyte proliferation. CDK9 is therefore a potentially important pathway that merits further evaluation as a therapeutic target.

In this study, we modulated CDK9, both genetically and pharmacologically, in the zebrafish embryo. We show that genetic knockdown and pharmacological inhibition of CDK9 inhibits cardiomyocyte proliferation, reduces cardiac function and the cardiac recovery ability following cardiac laser injury. Conversely, genetic inhibition of LARP7, a CDK9 repressor, provoked both a hyperplastic and hypertrophic cardiac response with preservation of cardiac function following injury and rescued the effects of CDK9 knockdown.

RESULTS

CDK9 and LARP7 expression display a distinct pattern in whole larvae and in isolated larval hearts during normal development

CDK9 was detected in normal whole larvae from 24 hours post fertilization (hpf) and showed a distinctive pattern of expression during the course of development increasing between 24 and 72 hpf ($p<0.01$) and then decreasing towards 120 hpf (Fig. 1A). In pooled-isolated embryonic hearts (n=150 per sample, n=3 samples) CDK9 mRNA peaked at 48 and again at 96 hpf, decreasing at 120 hpf to levels then detected in adult isolated hearts. CDK9 was also detectable at moderate levels (relative to embryonic) in the adult heart (Fig. 1B). In whole larvae, LARP7 expression reached a peak at 48 hpf and then decreased towards 72, 96 and 120 hpf (Fig. 1C). In isolated embryonic hearts, LARP7 mRNA increased slightly between 48 and 96 hpf and then reduced at 120 hpf. In the adult heart, LARP7 mRNA was also detectable (Fig. 1D).

Survival and gross phenotype of pharmacological and CDK9 morpholino treated larvae

Incubation of embryos in flavopiridol at time points less than 24 hpf resulted in high levels of mortality and so we used continuous incubation from 24 hpf which resulted in a modest reduction in survival in treated embryos compared to controls at 120 hpf (77±3% vs 91±4% respectively, p=ns, Fig. S1A).

Absence of heart beat, lack of tail blood flow combined with other major structural malformations were the criteria used to evaluate mortality. These larvae also displayed an excess of body axis deformities, small head, pericardial oedema and reduced tail blood flow. Flavopiridol had no significant effects on the anatomical configuration of the heart (Fig. 3C).

CDK9-Mo-TB (ATG translation blocking) treatment resulted in a significant reduction in survival compared to controls at 120 hpf (47±4,5% vs 85±4% respectively, $p<0,001$, Fig. S1B). In contrast, CDK9-Mo-SB (splice blocking) treatment was associated with a higher level of survival compared to controls (72±5% vs 85±4% respectively, p=ns). CDK9-Mo treated larvae displayed an excess of developmental and structural abnormalities, compared to controls, including deformity of trunk and tail curvature, small head, pericardial oedema, reduced tail blood flow and global developmental delay compared with controls (Fig. S2). These abnormalities were less frequent with CDK9-Mo-SB compared to CDK9-Mo-TB. This is a fairly typical observation since translation blocking Mo are known to inhibit both maternal and zygotic transcripts (Nasevicius and Ekker, 2000), whereas splicing blocking Mo are only active on zygotic transcripts. Due to the high mortality associated with the CDK9-Mo-

TB, we preferentially used embryos treated with CDK9-Mo-SB, which showed a similar degree of CDK9 protein knockdown, during the majority of the laser injury and rescue experiments to avoid the confounding issue of selection-survival bias.

Effects of CDK9 inhibition on CDK9 gene transcription, protein expression and phosphorylation of Ser2-CTD

Flavopiridol treatment caused a reduction in the levels of the phosphorylated form of the serine 2 residue of the CTD (carboxy-terminal domain) in whole larvae compared to controls (Fig. 2A, B, C) as predicted by its known pharmacological action (Chao et al., 2000, Bosken et al., 2014). However, Flavopiridol treated embryos, unexpectedly, showed an increase in CDK9 protein in whole larvae at 72 and 96 hpf (Fig. 2B,C).

Larvae injected with CDK9-Mo-SB showed a marked reduction in the abundance of CDK9 mRNA by over 70% as expected with morpholino treatment (Fig. 2D). This resulted in about 20% reduction in the levels of CDK9 protein at 48 and 96 hpf (Fig. 2E and F). This reduction in CDK9 protein was confirmed with both splice and translation blocking morpholinos (Fig. 2F).

CDK9 inhibition reduces size and function of the ventricle

During normal development zebrafish larvae show a progressive increase in ventricle size, measured as diastolic area, in the period 72-120 hpf. Ejection Fraction (EF) of the ventricle does not change during normal development. However, the increase in heart rate and cardiac size results in an increase in cardiac output. Pharmacological inhibition of CDK9 with flavopiridol from 24 hpf reduced ventricle size and EF compared to controls (Fig. 3A), although flavopiridol did not impact significantly on the anatomical structure of the heart (Fig. 3C). CDK9-Mo-SB had a marked effect on cardiac structure during development with a high proportion of hearts showing a string-like appearance by 120 hpf (Fig. 3B,C). These hearts were also significantly smaller and displayed reduced EF (Fig. 3B).

LARP7 morpholino causes a mild cardiac phenotype with enhanced phosphorylation of Ser2-CTD

Larvae injected with LARP7-Mo (either SB or TB) displayed similar rates of survival at 120 hpf to mismatch injected controls (90%) (Fig. S1C) with mild structural and cardiac abnormalities (see Fig. 4A and Fig. S3). Ventricle diastolic area and EF were not different between the two groups (Fig. 4B, C), whereas atrial diastolic area was significantly greater in LARP7-Mo injected embryo hearts compared to controls (Fig. 4D). LARP7-Mo-SB injected larvae

had a significant reduction in LARP7 mRNA by approximately 40% (Fig. 4E) and a reduction in LARP7 protein by 70% (Fig. 4E, F) compared to controls. LARP7-Mo-TB larvae showed an increase in P-Ser2-CTD compared to mismatch-controls (Fig. 4F) consistent with activation of CDK9.

Effects of CDK9 modulation on cardiomyocyte proliferation

Total number of ventricle cardiomyocytes (VC*t*) increased progressively during development in controls. Larvae exposed to flavopiridol 3 μmol/L (μM) (Fig. 5A) showed reduced VC*t* during this same developmental time period. Larvae treated with CDK9-Mo-SB also showed significantly lower VC*t* compared to mismatch controls with a reduction of 25%, 48% and 70% respectively at 72, 96 and 120 hpf (Fig. 5B). We ensured that only dividing cardiomyocytes were included in the counting process by carefully confirming that each PhosphoHistone H3 (PHH3) positive nucleus co-localized with DAPI and GFP signal. Exposure to flavopiridol 3 μmol/L (μM) significantly reduced the number of mitotic cardiomyocytes (Fig. 5D, E). The ratio of mitotic/total cardiomyocytes at 72 hpf was 2.8% in flavopiridol treated embryos compared to 5.5% in controls, corresponding to a 55% reduction in the number of PHH3 positive nuclei. In contrast, LARP7-Mo showed an increased number of VC*t* at 120 hpf compared to mismatch controls (Fig. 5C).

CDK9 modulation modifies GATA family mRNA abundance in whole larvae

Whole larvae (48 hpf) incubated in flavopiridol showed a reduction in the mRNA levels of *gata4* by 48 hpf with no change in *gata5* and *gata6* at this developmental stage (Fig. 6A). Whereas at 96 hpf larvae treated with flavopiridol showed an increased level of all GATA family mRNA, with values of 1.5±0.2 for *gata4*, 1.4±0.18 for *gata5* and 1.49±0.3 for *gata6*. Larvae treated with CDK9-Mo-SB did not show a difference in *gata4* and *5* at 48 and 96 hpf (Fig. 6B), whereas there was a reduction in *gata6* mRNA abundance at 96 hpf. Larvae treated with LARP7-Mo-TB showed no significant changes in the abundance of mRNA levels for *gata4-6* at 48 or 96 hpf (Fig. 6C).

CDK9 inhibition impairs recovery from cardiac laser injury

In control larvae, laser injury of the ventricle at 72 hpf resulted in a significant reduction in ejection fraction (EF) and total ventricular cardiomyocyte number (VC*t*) at 2 h post-laser (Fig. 7). By 24 h post-laser both parameters recovered to baseline levels comparable to those before laser injury.

Larvae exposed to flavopiridol or injected with CDK9-Mo-SB also showed a reduction in EF and VC*t* at 2 hours post-laser, however both parameters failed to recover to control levels by 24 h post-laser (figure 7).

Larvae treated with LARP7-Mo-TB (and SB) showed a significant reduction in EF and VC*t* values at 2 hours post-laser with recovery to control levels by 24 hours post-laser (Fig. 7).

Co-injection of LARP7-Mo and CDK9 capped RNA attenuates the morphological phenotype in CDK9-Mo treated larvae and restores functional recovery of the ventricle following laser injury

Co-injection of larvae with CDK9-Mo-SB and LARP7-Mo-SB significantly attenuated the morphological abnormalities observed with CDK9-Mo-SB alone with fewer embryos displaying body axis and cardiac abnormalities (Fig. 8A,B,C). Co-injection of CDK9-Mo and CDK9-RNA also significantly rescued the morphological phenotype observed with CDK9-Mo alone (Fig. 8A,B,C). There were significantly fewer larvae with small head, curved tails, string-heart and absent tail blood flow. While the rescue with CDK9 capped RNA did not completely restore the phenotype to normal we observed a substantial improvement in the structural and functional cardiac phenotype (Fig. 8C).

Following laser injury, co-injection of either CDK9-mRNA (capped) or LARP7-Mo-SB both enhanced recovery from laser injury with EF restored to normal in both co-injected embryo-sets within 24 hours (Fig. 8D). This compared favourably with the CDK9-Mo-SB injected larvae which showed persistently depressed EF at 24 hours after laser injury.

DISCUSSION

The zebrafish embryo provides a unique opportunity to assess the role of CDK9 in cardiomyocyte proliferation by using a highly accurate method of counting cardiomyocytes in whole embryonic ventricles combined with detailed structural and functional assessment of hearts at baseline and after laser-induced injury. We provide evidence that CDK9 plays a key role in early cardiac development and in cardiomyocyte proliferation. We have shown that CDK9 action can be pharmacologically inhibited resulting in dephosphorylation of its target site on the carboxyterminal domain (CTD) of the RNApol II. Knockdown of CDK9 transcription using morpholino technology also resulted in reduced CDK9 protein expression leading to reduced phosphorylation of its target site. We have shown that even a modest reduction (about 20%) of CDK9 protein, insufficient to cause significant structural or developmental abnormalities, has a striking effect on the embryonic heart with reduced size and function and a reduced capacity to recover from injury. In contrast, enhancing CDK9 activity by knockdown of its repressor molecule, LARP7, increased cardiomyocyte proliferation and was associated with a normal recovery of the ventricle from laser injury. These findings highlight the importance of CDK9 in the developing heart and its response to injury. Therefore, CDK9 represents a fundamental cellular mechanism in the heart controlling transcription and proliferation and point to its potential importance as a therapeutic target.

Molecular pathways linked to CDK9 appear to be more strongly associated with cell growth than control of cell cycle where other members of the CDK family have greater influence. Previous work has demonstrated that a dominant-negative CDK9 blocks ET-1-induced hypertrophy in cultured mouse cardiomyocytes (Sano et al., 2002) confirming a key role in cardiac hypertrophy.

CDK9 During Embryonic Development

In the mouse, cardiac CDK9 activity is highest during embryonic stages (E16.5) falling by 50% in the neonate and further still to around 15%, of embryonic levels by early adulthood (Sano et al., 2002). In the zebrafish heart, q-PCR analysis suggests that CDK9 is most strongly expressed during the first 96 hpf of development consistent with active cardiomyocyte proliferation. Thereafter, mRNA levels fall only modestly, by around 30%, remaining at around 70% of embryonic expression levels into adult life. This apparent difference could reflect the higher level of cardiomyocyte cell turnover in the zebrafish heart compared with the mouse (Soonpaa and Field, 1998).

Although the mechanisms of cell-cycle regulation are broadly conserved, the existence and function of CDK9 in the zebrafish has not been well described. One of the key aspects of our study was to establish that CDK9 was present and functional in the larval heart and to characterise its role in normal development. Inhibition of CDK9 using flavopiridol produced a significant decrease in the CDK9 activity assessed by phosphorylation of its target site P-Ser2 on the CTD. Injection of CDK9-targeting morpholino also resulted in a reduced CDK9 expression. These findings confirmed that CDK9 involves the same pathway in the zebrafish as it does in mammalian systems (Nguyen et al., 2001). CDK9 Morpholino treatment produced a number of phenotypic traits which were generally more severe than those observed with flavopiridol treatment, possibly reflecting differences in the time of onset of the two forms of treatment during development. Cardiovascular function was affected in both cases, with a reduction in cardiomyocyte proliferation, ventricle EF and tail blood flow.

Inhibition of CDK9

CDK9 inhibition is currently being evaluated in pre-clinical and clinical studies for the treatment of a number of different cancers mainly in combination with other chemotherapeutic agents (Hofmeister et al., 2014, Karp et al., 2010). While it has been proposed as a treatment for severe cardiac hypertrophy, there are no published trials and no evidence of any ongoing trials of its use in this clinical setting. The proposed mode of therapeutic action of CDK9-inhibitors in cardiac hypertrophy is inhibition of RNA and protein synthesis by limiting gene transcription.

In our study, Flavopiridol initially caused a marked reduction in phosphorylation of its target site on the CTD of RNApol II (Fig. 2A, C). This effect was relatively transient despite continuous exposure to the drug with normalisation of phosphorylation by 96 hpf. Simultaneously there was an unexpected and progressive increase in the levels of CDK9 protein between 48 and 96 hpf despite ongoing exposure to the drug (Fig. 2B, C). The lack of specific antibodies for the zebrafish total RNA Pol II did not allow us to fully exclude the possibility that the levels of RNA Pol II also changed under our experimental conditions. We observed a small non-significant rise in CDK9 mRNA abundance at 96 hpf following flavopiridol treatment. Taken together these findings suggest that the initial effect of flavopiridol changed with time, possibly due to tolerance or desensitisation and possibly also due to alternative or redundant CDK pathways providing phosphorylation of the target site. The increase in CDK9 protein levels is interesting and may be the result of a feedback mechanism which ensures ongoing and adequate phosphorylation of the CTD on RNApol II to maintain RNA transcription and elongation. Postulating such a mechanism is not unreasonable given the fundamental im-

portance of this pathway to basic cellular function. To our knowledge this is the first evidence of a feedback mechanism linking CDK9 and its phosphorylation target on RNApol II.

Flavopiridol also reduced mRNA abundance of *gata4* in the early stages of development and then later, towards 96 hpf, it produced an increase in the whole *gata* family including *gata4, 5* and *6*. This finding is somewhat counter-intuitive since these transcription factors are widely recognised as drivers of cardiomyocyte proliferation which was also observed to be adversely affected by flavopiridol. *gata4* in particular plays a key role in a number of signaling pathways in the heart and is known to be activated following haemodynamic stress (Cappola, 2008). Of specific interest is the fact that *gata4* has been shown to form a complex with CDK9, promoted by the intrinsic histone acetyl-transferase p300 that is also required for the kinase activity of CDK9. This complex is in turn required for transcriptional pathway activation during cardiomyocyte hypertrophy (Sunagawa et al., 2010). Despite the increasing levels of *gata4, 5* and *6* at 96 hpf, cardiomyocyte proliferation did not increase significantly. One possible explanation is that these three transcription factors play a dominant role in cardiomyocyte proliferation very early in the heart development (6-24 hours) whereas later in development (24-48 hours) other factors are more important in orchestrating the proliferative process.

Enhancing CDK9 activity

LARP7 specifically binds to and enhances the stability of the complex 7SK snRNA-HEXIM-CDK9 leading to repression of its action on RNA polymerase II. Knockdown of LARP7 would be expected to destabilise this complex leading to an increase in CDK9 activity. In contrast to CDK9 inhibition (either by flavopiridiol or direct CDK9 morpholino knockdown), LARP7 knockdown provoked an increase in ventricle cardiomyocyte number that was not associated with an increase in the ventricle size. This suggests a predominantly hyperplastic response. There was no change in ejection fraction of the ventricle although we did observe a consistent increase in dimensions of the atrium. The cause for is not clear and a contribution due to altered ventricular chamber stiffness could have played a role.

Response to laser injury

Cardiac injury is widely recognised to cause a switch of specific genetic and epigenetic programs (Bergmann and Steller, 2010, Dilworth and Blais, 2011, King and Newmark, 2012, Monaghan et al., 2012, Wang et al., 2012) including zebrafish (Kizil et al., 2012). The model used here involving targeted laser of the embryonic ventricle has similarities to myocardial infarction models in mammals i.e. it generates a sudden loss of myocardial tissue in a regional

distribution. It is highly reproducible and permits the study of both injury and recovery in a very short time period of 24 hours. By 2 hours after laser injury there is markedly reduced cardiac function accompanied by a reduced number of cardiomyocytes and increased apoptosis in the area of injury (Matrone et al., 2013). This functional loss recovers fully within 24 hours. Inhibition of CDK9 activity, with either flavopiridol or CDK9-Mo, resulted in reduced capacity of the ventricle to recover from injury. This failure to recover was associated with diminished cardiomyocyte proliferation. While loss of CDK9 action may have influenced a wide range of gene transciption pathways, including apoptosis pathways (Sano et al., 2004), the observed persistent cardiac dysfunction may have been significantly affected by the observed reduction in cardiomyocyte proliferation. Since CDK9 knockdown caused a persistent reduction in *gata4,5* and *6*, recognised proliferative transcription factors in the heart, we hypothesised that LARP7 knockdown would increase the number of cardiomyocytes. We also hypothesised that this approach would enhance the ability of the ventricle to recover from injury. We showed very clearly that the ventricles of LARP7-Mo treated embryos had increased numbers of cardiomyocytes at 120 hpf. Subsequently we showed that we could rescue the CDK9-Mo baseline phenotype with both CDK9 RNA and also by co-injecting with LARP7-Mo. We also showed that co-injection of LARP7-Mo reversed the effects of CDK9-Mo, permitting the embryonic heart to retain its capacity to recover fully from laser injury. As part of a set of validation experiments we co-injected CDK9 targeting morpholino with the mismatch LARP7 morpholino. This co-injection did not rescue the embryo phenotype. Only the co-injection of the CDK9 and LARP7 targeting morpholinos rescued the CDK9 morpholino embryonic phenotype. In addition, we prepared the solution immediately before the injection, to reduce as much as possible the formation of non-specific complexes. However, we cannot completely exclude the possibility of non-specific complex formation intefering with the action of the CDK9 Mo. LARP7 knockdown alone did not significantly affect cardiac recovery from laser injury.

The extent of CDK9 protein knockdown resulting from morpholino treatment was around 20% indicating ongoing availability of CDK9 to be modulated. In addition, the dynamic sharing of CDK9 between the two complexes in which CDK9 is involved, *i.e.* the CDK9/Cyclin active fraction and CDK9/LARP7-Hexim1/2-7SK inactive fraction, represents a functional balance that can be perturbed. Indeed, we believe that following LARP7 knockdown, more CDK9 enzyme is released from the inactive complex leading to increased activity. In mammals, the inactive P-TEFb complex includes HEXIM and 7SK and co-inhibiting two or more

of these CDK9 repressors could provide additional approaches to this mechanism as a possible short term therapeutic approach to enhance recovery from injury in the heart.

However, forcing mammalian cardiomyocytes to re–enter the cell cycle could activate mechanisms controlling inappropriate cell cycle entry in otherwise quiescent cells. For instance, a foreseeable obstacle to this approach in cardiomyocytes is that E2F-1, that provoke G1 exit and DNA synthesis (Kirshenbaum et al., 1996), could also induce cardiomyocyte p53-dipendent (Kowalik et al., 1995) or independent (Agah et al., 1997) apoptosis.

In this case, therapeutic interventions should include *ad hoc* modulation of antiapoptotic genes such as BCL-2 (Kirshenbaum and de Moissac, 1997).

Clearly further understanding of the factors and pathways controlling CDK9 activity is required. However, these pathways clearly merit further study as a possible therapeutic strategy to address diseases associated with acute and chronic heart injury.

Future perspectives

Our findings, while limited to the zebrafish embryonic heart, have refocused on the importance of CDK9 as a potential therapeutic target for human disease. There is clearly a need for further studies in mammalian cardiac model systems. A first step would be exploring CDK9 expression patterns in neonatal versus adult hearts and analysing its role in regenerative capacity (Porrello et al., 2011). It would also be very important to understand whether a heart specific CDK9 isoform exists, which would permit development of drugs targeted at CDK9's action in the heart thus avoiding off-target effects. Derepression of CDK9 by LARP7 knockdown or inhibition is an intriguing approach and one which could promote cell survival and enhance proliferation. While this would have potential carcinogenesis, short term use during periods of acute injury, such as myocardial infarction, merit further study.

In conclusion, we have shown that CDK9 and its repressor LARP7 can be modified to impact on cardiac growth and development specifically impacting on cardiomyocyte proliferation. Short term derepression of CDK9 represents an unexplored mechanism with the potential to promote functional recovery of the heart following injury via a mechanism associated with enhanced cardiomyocyte proliferation.

MATERIAL AND METHODS

Ethical approval

All experiments were approved by the local ethics committee and conducted in accordance with the United Kingdom Animals (Scientific Procedures) Act 1986 in an approved establishment.

Zebrafish maintenance

Zebrafish husbandry, embryo collection and maintenance were performed according to accepted standard operating procedures (Nüsslein-Volhard, 2002). The cardiac myosin light chain 2:GFP transgenic line (Tg(cmlc2:GFP)) (Burns et al., 2005) was used for all experiments; larvae were maintained at 28.5°C on a 14 h light/10 h dark cycle and staged according to Kimmel (Kimmel et al., 1995). Larvae were maintained in egg water until dechorionated and then in embryo medium (Westerfield, 2000). Embryos were anesthetized in a solution of Tricaine 20 µmol/L (µM) (ethyl 3-aminobenzoate methanesulfonate, SIGMA) or euthanised with an overdose of the same compound. All experimental procedures were performed at room temperature (RT, 23°C).

Morpholino injections

Suppression of CDK9 and LARP7 expression was achieved using antisense morpholino (Gene Tools, Oregon, USA) designed against the splice donor between exon 3 and intron 3, or targeting the mRNA AUG translational start site.

Morpholino (Mo) sequences were as follows: CDK9-Mo splice blocking (sb) ((NM_212591.1) 5'-CTTTCTTCCCCATTCTTTTACGTGG-3'), CDK9-Mo translation blocking (tb) (5'-CCTACGTCGCGCTGTTTTGGCCTTC-3'), CDK9 control mismatch Mo (5'-CTTTgTTgCCgATTgTTTTACcTGG-3'), LARP7-Mo sb (NM_199930.1, 5'-TCATCTCCATACTAAACCAAACTGT-3').

LARP7 Mo tb (5'-TACTTTCACACAGTTGCGTTCTGCT-3'), LARP7 control mismatch Mo (5'-TgATgTCCATAgTAAACgAAACTcT-3').

A 0.5 nanolitre of morpholino solution (100 µmol/L (µM) for CDK9 and 200 µmol/L (µM) for LARP7) was injected in one to two-cell stage larvae, just beneath the blastoderm using a pulled glass pipette using a standard injector (IM300 Microinjector, Narishige, Japan). Successful injection was assessed under fluorescence microscope by the red tag lissamine at the 3'end of the morpholino oligos.

CDK9 Morpholino Rescue by CDK9 mRNA

To determine whether the effect of the CDK9 morpholino was specifically due to loss of CDK9 we performed a rescue experiment by co-injecting CDK9-Mo with capped CDK9 RNA. This capped RNA was produced using an IMAGE clone encoding *D. Rerio* CDK9 cDNA (Source Bioscience, Cambridge, UK) which was sub-cloned into pNR-LIB (Source Bioscience, Cambridge, UK). Following linearization with XhoI restriction enzyme (Applied Biosystems, New York, USA), capped CDK9 RNA was transcribed using an mMessage mMachine Kit (Ambion, New York, USA) according to the manufacturer's instruction. A bolus of 1 nL of solution containing CDK9 morpholino 100 µmol/L (µM) and 1.25 ng of CDK9 RNA was injected in each egg.

CDK9 Morpholino Rescue by LARP7 knockdown

Co-injection of CDK9-Mo SB and LARP7-Mo was performed to assess whether the phenotype and the response to laser injury observed in CDK9-Mo larvae could be rescued by LARP7 knockdown. A bolus of 1 nL of solution containing CDK9 morpholino 100 µmol/L (µM) and LARP7 morpholino 200 µmol/L (µM) was injected in each egg.

Pharmacological treatment of larvae

Flavopiridol is recognized as a potent ATP competitive kinase inhibitor for CDK9 (Bosken et al., 2014, Baumli et al., 2008), that is now in clinical trials (Wang and Fischer, 2008). Zebrafish larvae (24 hpf) were placed in embryo medium containing flavopiridol 3 µmol/L (µM) (Sigma, Suffolk, UK) diluted in 1% DMSO. Solutions were replaced at 48, 72 and 96 hpf. Control embryos were exposed at DMSO 1%. The drug concentration of 3 µmol/L was selected after a series of experiments assessing the concentration of flavopiridol which resulted in minimum toxicity to the whole embryo while also resulting in a significant decrease in CDK9 activity confirmed by reduced phosphorylation of the serine 2 residue of RNA polymerase II.

Assessment of ventricular function

Video images of the beating heart were captured by video camera (IonOptix CCD100 MyoCam^{tm}, Dublin, Ireland), mounted on a microscope (Axioscope II MOT Plus, Zeiss) linked to a computer. Ventricle end-systolic and end-diastolic area were measured using image analysis software (ImageJ, NIH, Bethesda). Fractional-area change (Ejection fraction, EF) was estimated by subtracting ventricular systolic area from diastolic area, expressed as a percentage of diastolic area, as previously described (Shu et al., 2003).

Histology and Ventricle Cardiomyocyte number

Total ventricular cardiomyocyte number (VC*t*) and proliferating ventricular cardiomyocyte number (VC*p),* counted as DAPI and PHH3 positive nuclei respectively, were assessed in whole-mount isolated embryonic hearts, as previously described (Matrone et al., 2015). Larvae were euthanized in Tricaine 1mM and fixed in 4% paraformaldehyde (PFA, Sigma). Microdissected hearts were pre-incubated in proteinase K (10 µg/ml) to allow permeabilization, washed in PBS and Triton-X100 (0.1%) and then blocked in Bovine Serum Albumin 5% in PBS for 3 h) before being incubated with anti-PHH3 antibody (Millipore 05-670; rabbit, 1:200), followed by incubation with anti-rabbit antibody (Alexa fluor, Dako, 1:500). Subsequently, hearts were incubated in DAPI (Sigma, 1:1000) for 1 h, washed in PBS and then mounted in glycerol 100%. Confocal microscopy (Leica SP5) was used to capture z-stack images of isolated heart ventricles at 3 µm intervals. The total number of ventricular cardiomyocytes (VC*t*) and the number of mitotic ventricular cardiomyocytes (VC*p*) were counted using ImageJ software, by marking each nucleus with a tag while moving progressively through the z-stack. Only cardiomyocytes were included in the counting process by ensuring that each nucleus was located within a GFP positive region of the heart. The atrium and bulbus arteriosus were excluded from counting. Counting was performed by a single individual blinded to the original treatment of the heart. Intra-observer variation for a sample of 25 hearts was ±4.5%.

Haematoxylin & Eosin (H&E) staining of whole larvae was performed. Serial 4 µm sagittal sections were stained according to standard protocols (Sabaliauskas et al., 2006).

Heart laser injury

Laser-injury of the Zebrafish embryonic heart was induced using a XYclone Laser (Hamilton-Thorne, USA) using the technique previously reported by our group (Matrone et al., 2013). The protocol for laser injury and recovery is summarised in Fig. S4. Briefly, larvae 72 hpf were anaesthetised using Tricaine 20 µmol/L (µM) (SIGMA) and placed on a plain glass microscope slide in a minimal amount of water. Under standard white light microscopy (Axioscope II MOT Plus, Zeiss), a laser pulse was delivered to the midpoint of the ventricle (see movie S1). The average energy delivered per pulse was 0.9 mJ over a duration of 3 ms (300 mW) directed at an area approximately 10 µm in diameter. After injury, each embryo was immediately placed in embryo medium to recover for a further 48 h. Controls larvae, kept in identical conditions and manipulated in the same way, received laser injury to the distal tail-fin.

Gene expression

Quantitative real time PCR (Q-PCR) was used to assess the mRNA levels of CDK9, LARP7, GATA4, 5 and 6, following morpholino injection or flavopiridol exposure.

RNA extraction and reverse transcription were performed by using Qiagen RNeasy mini kit (Qiagen, West Sussex, UK).

Larvae were placed in an eppendorf tube 1.5mL, euthanised with tricaine overdose and stored in RNAlater (Life Technologies Ltd, Paisley, UK) or, for immediate RNA extraction, placed directly in buffer RLT 600 µL. Each Eppendorf tube was added with two small metallic bead, previously autoclaved and wiped with RNase Zap (Life Technologies Ltd, Paisley, UK). Efficient disruption and homogenization was performed by milling for 45 s at 30 Hz (Mixer Mill 301 model, Retsch, Haan, Germany) while maintaining the larvae homogenate cold at all times. Beads were removed and the samples were centrifuged at 13,000g, 3 mins, 4°C. The supernatant was placed in a new 2 mL Eppendorf tube and the pellet discarded. Supernatant was added with an equal volume of 70% ethanol, mixed and placed in the RNeasy spin column subjected to centrifugation (12,000g, 30 s, 4°C). The eluate was discarded.

DNase treatment step followed to eliminate genomic DNA contamination. After wash with Buffer RW1 (350 µl) and centrifugation for 15 s, 10 µl DNase I stock solution, previously diluted in 70 µl Buffer RDD, were added to the spin column and incubated 15 mins at RT. The column was then washed with Buffer RW1 (700 µl) and Buffer RPE (500 µL). In each case, the eluate was discarded following centrifugation (12,000g, 15 s, 4ºC). Buffer RPE (500 µl) was added to wash the membrane, followed by a further centrifugation step (12,000g, 2 mins, 4ºC). The spin column was then placed in a fresh 2 mL collecting tube and subjected to centrifugation (16,000g, 1 min, 4ºC) to eliminate any Buffer RPE carryover. The spin column was then placed in a fresh 1.5 mL eppendorf, RNase-free water (30 µl) added and RNA eluted by centrifugation (12,000g, 1 min, 4°C). Eluted RNA was stored at -80°C.

RNA was quantified using a Nanodrop Spectrophotometer (Thermo Fisher, West Sussex, UK) in 1 µl of RNA sample. Concentration was determined by the absorbance at 260 nm wavelength (A260), and the purity assessed by the ratio of RNA/DNA (A260/A280), which was deemed acceptable if between 1.9 and 2.1, and 260/230 (some contaminants, e.g. phenol, absorb at 230nm) > 2.2.

Quality of RNA was assessed by electrophoresis on agarose (Lonza, Berkshire, UK) gel (1% w/v in 0.5x TBE). Samples (2µl) were prepared by adding loading dye (Promega, WI, USA;) 1 in 5 diluted in distilled water. Sample were incubated at 85°C for 3 min to denature RNA before running on the gel (100V, 1hr) with a size marker (New England Biolabs, MA,

USA). RNA integrity was assessed on basis of 18S and 28S ribosomal RNA (rRNA) bands. RNA integrity was deemed satisfactory if clear 28S and 18S rRNA bands were present without smearing, and if 28S rRNA band was approximately twice as intense as 18S rRNA band.

RNA was reverse transcribed in cDNA by using high capacity cDNA reverse transcription kit (Applied Biosystems, Warrington, UK).

For each sample, a volume containing 2 µg of RNA was pipetted in a 0.2 mL microfuge, added with nuclease free water up to 10 µl and then another 10 µl of RT master mix (2x) was added. Two negative controls were prepared as above, one with water instead of RNA to identify any RNA contamination in reagents, the second without the reverse transcriptase enzyme in order to detect the presence of contamination by genomic DNA. Samples were incubated (25°C, 10 min; 37°C, 120 mins; 85°C, 5 mins; 4°C, ∞) in a PCR machine, before being chilled to 4°C. The resultant cDNA was stored at -20°C.

To enable quantitation of gene expression, two housekeeping genes were chosen based on their stability in respective experiments. Ef1α was used during normal embryonic development whereas ß-actin was used during embryonic exposure to flavopiridol or treatment with Morpholinos.

Primers were designed to match probes within the Roche Universal Probe Library (https://www.roche-applied-science.com). cDNA samples were heated for initial denaturation (95ºC, 5min), then underwent 50 cycles of PCR amplification, which consisted of denaturation (95ºC, 10 sec), annealing (60ºC, 30 sec) and elongation (72ºC, 1 sec). Upon completion of the PCR program, samples were cooled (40ºC, 30 sec). For all the samples, amplification curves were plotted (y axis fluorescence, x axis cycle number). Triplicates were deemed acceptable if the standard deviation of crossing point (Cp) < 0.5 cycles. Relative quantitation was calculated using the delta CT method using Light Cycler software.

Protein analysis

Western blotting followed by densitometric quantitation of the membrane bands (ImageJ software; NIH, Bethesda) was used for semi-quantitative analysis of proteins. Anti-CDK9 antibody was produced in rabbit (C12F7, Cell Signalling Technology; 1:200 in PBS); anti-P-Ser2 was produced in mice (ab24758, Abcam, Cambridge, UK; 1:500 in PBS); anti-LARP7 was a synthetic peptide (AV40848, Sigma; 1:1000 in PBS). To correct for variations in the amount of total protein loaded on the gel, target proteins (CDK9, P-Ser2 or LARP7) were normalised to the protein β-tubulin (ab6046, Abcam).

Embryo chorion and yolk sac were surgically removed using fine forceps (Dumont #5). Dechorionated and deyolked larvae were transferred into fresh, cooled PBS solution and rinsed twice and transferred into an eppendorf tube 1.5 mL Samples were microfuged for 1-2 mins and supernatant was removed. About 100-150 µL RIPA Lysis Buffer (Millipore, MA, USA), previously diluted in deionized water from a stock 10X, were added and homogenized with a microfuge pestle for 30 s and then sonicated for 30 s at 5-8 µW, until embryo sample was no longer visible. Samples were kept in ice for 30 mins, then were briefly vortexed and then microfuged 1-2 mins at full speed (13,000 rpm). Supernatant was collected and then placed in a new 1.5 mL tube and pellet was discarded.

The protein concentrations of zebrafish larvae homogenates were determined colorimetrically using a Bio-Rad protein assay kit (Bio-Rad, Hemel Hempstead, UK) and the Bradford method of detection (Bradford, 1976).

An appropriate amount of protein sample containing 20 µg of total protein was taken in a fresh eppendorf tube and immediately added with 4 µl of 4X laemmli buffer and deionised water to make a final volume of 16 µl. Samples were mixed and heated at 95°C for 5 mins.

Samples were separated by electrophoresis on a NuPAGE® Novex® 4-12% Bis-Tris Gel 1.0 mm thick (Life Technologies Ltd, Paisley, UK). In addition to the samples, a 5 µl of Novex® Sharp Pre-stained Protein Standard (Life Technologies Ltd, Paisley, UK) was also loaded to identify the molecular weight of bands. Gels were run at a voltage 100 V for 30 mins and then at 150 V for another 60 mins.

Gels were transferred to nitrocellulose membranes Protran (Sigma-Aldrich Ltd., Dorset, UK) using the Electrophoretic Transfer Cell (Biorad Laboratories, Hercules, CA, USA). A gel sandwich was prepared within the cassette consisting of fiber pad, blotting paper (both from Bio-Rad Laboratories, Hercules, CA, USA), gel, nitrocellulose membrane, filter paper and fiber pad. The gel sandwich cassette was placed within the transfer module and tank, which was then filled with Towbin transfer buffer (TRIS 0.025 M, Glycine 0.192 M, pH 8.6 ± 0.1). The transfer was run at 100 V and 300 mA for about 3 h at 4 °C. Nitrocellulose was then stained in Red Ponceau (Sigma-Aldrich Ltd., Dorset, UK) for 5 mins and then washed in water to check the presence of protein, while the remaining gel was stained in Comassie Blue R-250 0.5% (Bio-Rad Laboratories, Hercules, CA, USA) for 1 h followed by several wash in decoloration solution to assess that a good transfer occurred.

After transfer, nitrocellulose membrane was blocked with 20 ml of 5% dried skimmed milk (Marvel Premier Brands Ltd., Lincolnshire, UK) in TBS Tween (20mM Tris-Cl [0.2 M Tris-Cl, pH 7.6], 137mM Sodium Chloride, 0.1% Tween 20 [Polyoxyethylenesorbitan

monolaurate, BDH, Poole, UK]) on a platform shaker for 1 hour at RT. Then the membrane was washed 3 times (5 mins each) with PBS-Tween 0,1% and then incubated in primary antibody at a concentration according to antibody manufacturer (usually 1:500 - 1:1000) in Bovine Serum Albumin (Sigma-Aldrich Ltd., Dorset, UK) 3% overnight at 4°C. The membrane was washed 3 times inn PBS-Tween 0,1% prior to incubation with a secondary antibody, linked to the horse radish peroxydase, at a concentration of 1:10000 in dried skimmed milk 5% for 1 h. A final series of washes was performed as above, before the blot was developed.

Nitrocellulose membrane was exposed for 1 min to the Enhanced Chemiluminescence solution (ECL; Amersham, UK) following the manufacturer's instructions. Excess ECL substrate from the membrane was removed by touching the edge of the membrane to a piece of tissue paper. Then the membrane was placed down on a film layer, previously disposed inside a film cassette. The bubbles were carefully removed from the membrane that was then covered with another film layer, fixed on the cassette with tape and exposed to a photographic film (BioMax XAR Film Kodak, Sigma-Aldrich Ltd., Dorset, UK) for an adequate exposure time. The film was developed and immunoreactivity (band density) was quantified by densitometry (online source: http://rsbweb.nih.gov/ij/docs/user-guide.pdf) using ImageJ.

Defining the whole embryo and cardiac phenotype

Whole embryo and cardiac phenotype following treatments and flowing rescue were described on the basis of morphologic and functional characteristics under bright field microscopy. Embryo phenotype was assessed using a simple 6 point scoring system – 1 point was allocated for each of the following features - normal heart rate, normal head shape and size, normal body axis, normal tail blood flow, absence of pericardial oedema and absence of blood pooling. If these were all normal in any single embryo then this animal was scored as 6. Further detailed phenotype characterization was undertaken independently within our laboratory for each of the three CDK9 manipulations. In addition to the above characteristics, this assessment also included body angle as a measure of developmental stage where 0-5% was considered normal, curved was 5-50% and marked curvature was >50%. At least 4 different clutches of larvae were assessed under each of the treatment groups.

Statistical analysis

Experiments were performed in triplicate with on average 20-30 larvae per experiment, unless otherwise stated. Data are presented as mean ± standard error of the mean (SEM). Statistical analyses were performed using GraphPad Prism 5. One-way or two-way repeated measures ANOVA followed by Bonferroni post-hoc test were used to compare means within and between groups. P values <0.05 were considered significant.

ACKNOWLEDGMENT

We are grateful to Calum McRae, Boston, for provision of the *myl7:GFP* zebrafish line and John P. Cooke, Methodist Hospital Research Institute, for critically reading the manuscript.

FUNDING STATEMENT

This work was supported by the British Heart Foundation Centre Core Award and Research Excellence award and the Medical Research Council (UK).

DISCLOSURES

None.

REFERENCES

AGAH, R., KIRSHENBAUM, L. A., ABDELLATIF, M., TRUONG, L. D., CHAKRABORTY, S., MICHAEL, L. H. & SCHNEIDER, M. D. 1997. Adenoviral delivery of E2F-1 directs cell cycle reentry and p53-independent apoptosis in postmitotic adult myocardium in vivo. *J Clin Invest,* 100**,** 2722-8.

AHUJA, P., SDEK, P. & MACLELLAN, W. R. 2007. Cardiac myocyte cell cycle control in development, disease, and regeneration. *Physiol Rev,* 87**,** 521-44.

BARBORIC, M., KOHOUTEK, J., PRICE, J. P., BLAZEK, D., PRICE, D. H. & PETERLIN, B. M. 2005. Interplay between 7SK snRNA and oppositely charged regions in HEXIM1 direct the inhibition of P-TEFb. *EMBO J,* 24**,** 4291-303.

BAUMLI, S., LOLLI, G., LOWE, E. D., TROIANI, S., RUSCONI, L., BULLOCK, A. N., DEBRECZENI, J. E., KNAPP, S. & JOHNSON, L. N. 2008. The structure of P-TEFb (CDK9/cyclin T1), its complex with flavopiridol and regulation by phosphorylation. *EMBO J,* 27**,** 1907-18.

BECKER, J. R., DEO, R. C., WERDICH, A. A., PANAKOVA, D., COY, S. & MACRAE, C. A. 2011. Human cardiomyopathy mutations induce myocyte hyperplasia and activate hypertrophic pathways during cardiogenesis in zebrafish. *Dis Model Mech,* 4**,** 400-10.

BERGMANN, A. & STELLER, H. 2010. Apoptosis, stem cells, and tissue regeneration. *Sci Signal,* 3**,** re8.

BOSKEN, C. A., FARNUNG, L., HINTERMAIR, C., MERZEL SCHACHTER, M., VOGEL-BACHMAYR, K., BLAZEK, D., ANAND, K., FISHER, R. P., EICK, D. & GEYER, M. 2014. The structure and substrate specificity of human Cdk12/Cyclin K. *Nat Commun,* 5**,** 3505.

BURNS, C. G., MILAN, D. J., GRANDE, E. J., ROTTBAUER, W., MACRAE, C. A. & FISHMAN, M. C. 2005. High-throughput assay for small molecules that modulate zebrafish embryonic heart rate. *Nat Chem Biol,* 1**,** 263-4.

CAPPOLA, T. P. 2008. Molecular remodeling in human heart failure. *J Am Coll Cardiol,* 51**,** 137-8.

CHAO, S. H., FUJINAGA, K., MARION, J. E., TAUBE, R., SAUSVILLE, E. A., SENDEROWICZ, A. M., PETERLIN, B. M. & PRICE, D. H. 2000. Flavopiridol inhibits P-TEFb and blocks HIV-1 replication. *J Biol Chem,* 275**,** 28345-8.

DI STEFANO, V., GIACCA, M., CAPOGROSSI, M. C., CRESCENZI, M. & MARTELLI, F. 2011. Knockdown of cyclin-dependent kinase inhibitors induces cardiomyocyte re-entry in the cell cycle. *J Biol Chem,* 286**,** 8644-54.

DILWORTH, F. J. & BLAIS, A. 2011. Epigenetic regulation of satellite cell activation during muscle regeneration. *Stem Cell Res Ther,* 2**,** 18.

GARRIGA, J. & GRANA, X. 2004. Cellular control of gene expression by T-type cyclin/CDK9 complexes. *Gene,* 337**,** 15-23.

HE, N., JAHCHAN, N. S., HONG, E., LI, Q., BAYFIELD, M. A., MARAIA, R. J., LUO, K. & ZHOU, Q. 2008. A La-related protein modulates 7SK snRNP integrity to suppress P-TEFb-dependent transcriptional elongation and tumorigenesis. *Mol Cell,* 29**,** 588-99.

HOFMEISTER, C. C., POI, M., BOWERS, M. A., ZHAO, W., PHELPS, M. A., BENSON, D. M., KRAUT, E. H., FARAG, S., EFEBERA, Y. A., SEXTON, J., LIN, T. S., GREVER, M. & BYRD, J. C. 2014. A phase I trial of flavopiridol in relapsed multiple myeloma. *Cancer Chemother Pharmacol,* 73**,** 249-57.

KARP, J. E., BLACKFORD, A., SMITH, B. D., ALINO, K., SEUNG, A. H., BOLANOS-MEADE, J., GREER, J. M., CARRAWAY, H. E., GORE, S. D., JONES, R. J., LEVIS, M. J., MCDEVITT, M. A., DOYLE, L. A. & WRIGHT, J. J. 2010. Clinical activity of sequential flavopiridol, cytosine arabinoside, and mitoxantrone for adults with newly diagnosed, poor-risk acute myelogenous leukemia. *Leuk Res,* 34**,** 877-82.

KIKUCHI, K., HOLDWAY, J. E., WERDICH, A. A., ANDERSON, R. M., FANG, Y., EGNACZYK, G. F., EVANS, T., MACRAE, C. A., STAINIER, D. Y. & POSS, K. D. 2010. Primary contribution to zebrafish heart regeneration by gata4(+) cardiomyocytes. *Nature,* 464**,** 601-5.

KIMMEL, C. B., BALLARD, W. W., KIMMEL, S. R., ULLMANN, B. & SCHILLING, T. F. 1995. Stages of embryonic development of the zebrafish. *Dev Dyn,* 203**,** 253-310.

KING, R. S. & NEWMARK, P. A. 2012. The cell biology of regeneration. *J Cell Biol,* 196**,** 553-62.

KIRSHENBAUM, L. A., ABDELLATIF, M., CHAKRABORTY, S. & SCHNEIDER, M. D. 1996. Human E2F-1 reactivates cell cycle progression in ventricular myocytes and represses cardiac gene transcription. *Dev Biol,* 179**,** 402-11.

KIRSHENBAUM, L. A. & DE MOISSAC, D. 1997. The bcl-2 gene product prevents programmed cell death of ventricular myocytes. *Circulation,* 96**,** 1580-5.

KIZIL, C., KYRITSIS, N., DUDCZIG, S., KROEHNE, V., FREUDENREICH, D., KASLIN, J. & BRAND, M. 2012. Regenerative neurogenesis from neural progenitor cells requires injury-induced expression of gata3. *Dev Cell,* 23**,** 1230-7.

KOWALIK, T. F., DEGREGORI, J., SCHWARZ, J. K. & NEVINS, J. R. 1995. E2F1 overexpression in quiescent fibroblasts leads to induction of cellular DNA synthesis and apoptosis. *J Virol,* 69**,** 2491-500.

KRUEGER, B. J., JERONIMO, C., ROY, B. B., BOUCHARD, A., BARRANDON, C., BYERS, S. A., SEARCEY, C. E., COOPER, J. J., BENSAUDE, O., COHEN, E. A., COULOMBE, B. & PRICE, D. H. 2008. LARP7 is a stable component of the 7SK snRNP while P-TEFb, HEXIM1 and hnRNP A1 are reversibly associated. *Nucleic Acids Res,* 36**,** 2219-29.

KRYSTOF, V., BAUMLI, S. & FURST, R. 2012. Perspective of cyclin-dependent kinase 9 (CDK9) as a drug target. *Curr Pharm Des,* 18**,** 2883-90.

KRYSTOF, V., CHAMRAD, I., JORDA, R. & KOHOUTEK, J. 2010. Pharmacological targeting of CDK9 in cardiac hypertrophy. *Med Res Rev,* 30**,** 646-66.

LOYER, P., TREMBLEY, J. H., KATONA, R., KIDD, V. J. & LAHTI, J. M. 2005. Role of CDK/cyclin complexes in transcription and RNA splicing. *Cell Signal,* 17**,** 1033-51.

MARKERT, A., GRIMM, M., MARTINEZ, J., WIESNER, J., MEYERHANS, A., MEYUHAS, O., SICKMANN, A. & FISCHER, U. 2008. The La-related protein LARP7 is a component of the 7SK ribonucleoprotein and affects transcription of cellular and viral polymerase II genes. *EMBO Rep,* 9**,** 569-75.

MATRONE, G., TAYLOR, J. M., WILSON, K. S., BAILY, J., LOVE, G. D., GIRKIN, J. M., MULLINS, J. J., TUCKER, C. S. & DENVIR, M. A. 2013. Laser-targeted ablation of the zebrafish embryonic ventricle: A novel model of cardiac injury and repair. *Int J Cardiol*.

MATRONE, G., WILSON, K. S., MULLINS, J. J., TUCKER, C. S. & DENVIR, M. A. 2015. Temporal cohesion of the structural, functional and molecular characteristics of the developing zebrafish heart. *Differentiation,* 89**,** 117-27.

MONAGHAN, J. R., ATHIPPOZHY, A., SEIFERT, A. W., PUTTA, S., STROMBERG, A. J., MADEN, M., GARDINER, D. M. & VOSS, S. R. 2012. Gene expression patterns specific to the regenerating limb of the Mexican axolotl. *Biol Open,* 1**,** 937-48.

NASEVICIUS, A. & EKKER, S. C. 2000. Effective targeted gene 'knockdown' in zebrafish. *Nat Genet,* 26**,** 216-20.

NGUYEN, V. T., KISS, T., MICHELS, A. A. & BENSAUDE, O. 2001. 7SK small nuclear RNA binds to and inhibits the activity of CDK9/cyclin T complexes. *Nature,* 414**,** 322-5.

NÜSSLEIN-VOLHARD, C., DAHM, R. 2002. *Zebrafish, A Practical Approach,* Oxford, Oxford University Press.

PORRELLO, E. R., MAHMOUD, A. I., SIMPSON, E., HILL, J. A., RICHARDSON, J. A., OLSON, E. N. & SADEK, H. A. 2011. Transient regenerative potential of the neonatal mouse heart. *Science,* 331**,** 1078-80.

POSS, K. D., WILSON, L. G. & KEATING, M. T. 2002. Heart regeneration in zebrafish. *Science,* 298**,** 2188-90.

SABALIAUSKAS, N. A., FOUTZ, C. A., MEST, J. R., BUDGEON, L. R., SIDOR, A. T., GERSHENSON, J. A., JOSHI, S. B. & CHENG, K. C. 2006. High-throughput zebrafish histology. *Methods,* 39**,** 246-54.

SANO, M., ABDELLATIF, M., OH, H., XIE, M., BAGELLA, L., GIORDANO, A., MICHAEL, L. H., DEMAYO, F. J. & SCHNEIDER, M. D. 2002. Activation and function of cyclin T-Cdk9 (positive transcription elongation factor-b) in cardiac muscle-cell hypertrophy. *Nat Med,* 8**,** 1310-7.

SANO, M., WANG, S. C., SHIRAI, M., SCAGLIA, F., XIE, M., SAKAI, S., TANAKA, T., KULKARNI, P. A., BARGER, P. M., YOUKER, K. A., TAFFET, G. E., HAMAMORI, Y., MICHAEL, L. H., CRAIGEN, W. J. & SCHNEIDER, M. D. 2004. Activation of cardiac Cdk9 represses PGC-1 and confers a predisposition to heart failure. *EMBO J,* 23**,** 3559-69.

SHU, X., CHENG, K., PATEL, N., CHEN, F., JOSEPH, E., TSAI, H. J. & CHEN, J. N. 2003. Na,K-ATPase is essential for embryonic heart development in the zebrafish. *Development,* 130**,** 6165-73.

SOONPAA, M. H. & FIELD, L. J. 1998. Survey of studies examining mammalian cardiomyocyte DNA synthesis. *Circ Res,* 83**,** 15-26.

SUN, X., HOAGE, T., BAI, P., DING, Y., CHEN, Z., ZHANG, R., HUANG, W., JAHANGIR, A., PAW, B., LI, Y. G. & XU, X. 2009. Cardiac hypertrophy involves both myocyte hypertrophy and hyperplasia in anemic zebrafish. *PLoS One,* 4**,** e6596.

SUNAGAWA, Y., MORIMOTO, T., TAKAYA, T., KAICHI, S., WADA, H., KAWAMURA, T., FUJITA, M., SHIMATSU, A., KITA, T. & HASEGAWA, K. 2010. Cyclin-dependent kinase-9 is a component of the p300/GATA4 complex required for phenylephrine-induced hypertrophy in cardiomyocytes. *J Biol Chem,* 285**,** 9556-68.

WANG, S. & FISCHER, P. M. 2008. Cyclin-dependent kinase 9: a key transcriptional regulator and potential drug target in oncology, virology and cardiology. *Trends Pharmacol Sci,* 29**,** 302-13.

WANG, X., TREDGET, E. E. & WU, Y. 2012. Dynamic signals for hair follicle development and regeneration. *Stem Cells Dev,* 21**,** 7-18.

WESTERFIELD, M. 2000. The Zebrafish Book: A Guide for the Laboratory Use of Zebrafish (Danio rerio). Univ. of Oregon Press, Eugene.

YIK, J. H., CHEN, R., NISHIMURA, R., JENNINGS, J. L., LINK, A. J. & ZHOU, Q. 2003. Inhibition of P-TEFb (CDK9/Cyclin T) kinase and RNA polymerase II transcription by the coordinated actions of HEXIM1 and 7SK snRNA. *Mol Cell,* 12**,** 971-82.

Figures

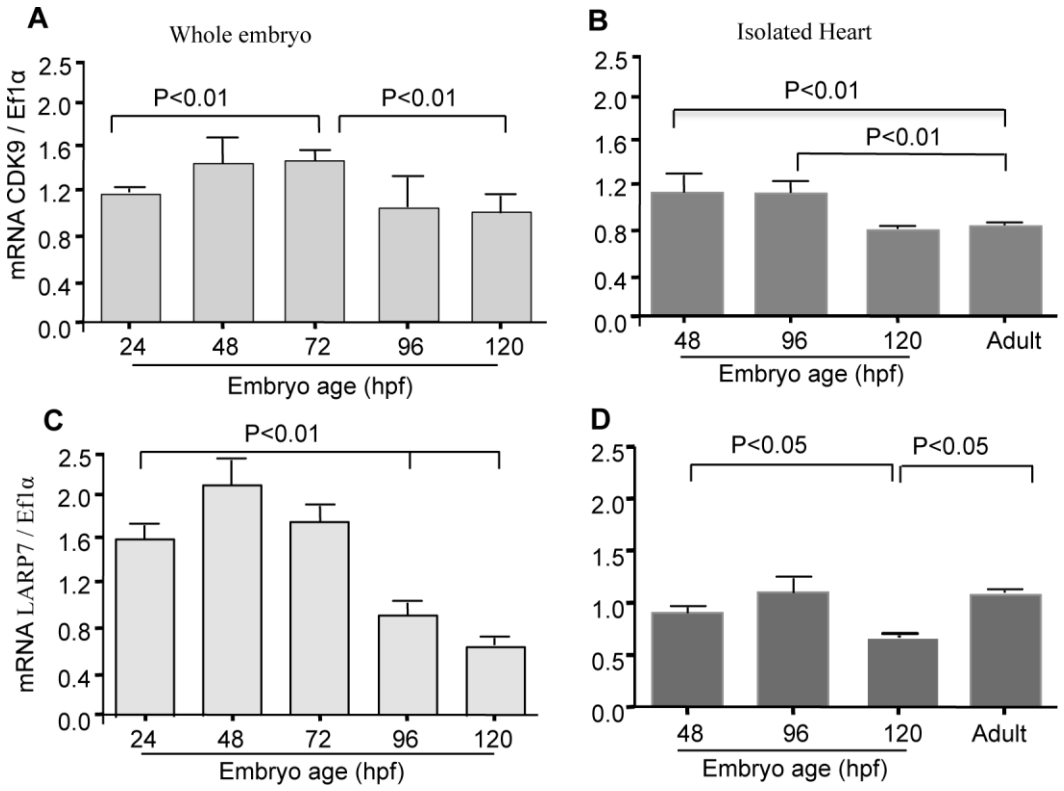

Figure 1- qPCR assessment of CDK9 and LARP7 gene expression in the whole embryo and in isolated zebrafish hearts.

CDK9 and LARP7 mRNA relative abundance in whole embryos collected from 24 to 120 hpf (**A, C**) and in isolated embryonic hearts at 48, 96, 120 hpf and adult heart (6 months age) (**B, D**). Data were compared using one-way ANOVA followed by Bonferroni's multiple comparison test. Each time-course was studied in 1 clutch of eggs with at least 10 embryos per time point. Mean values represents 3 clutches of eggs.

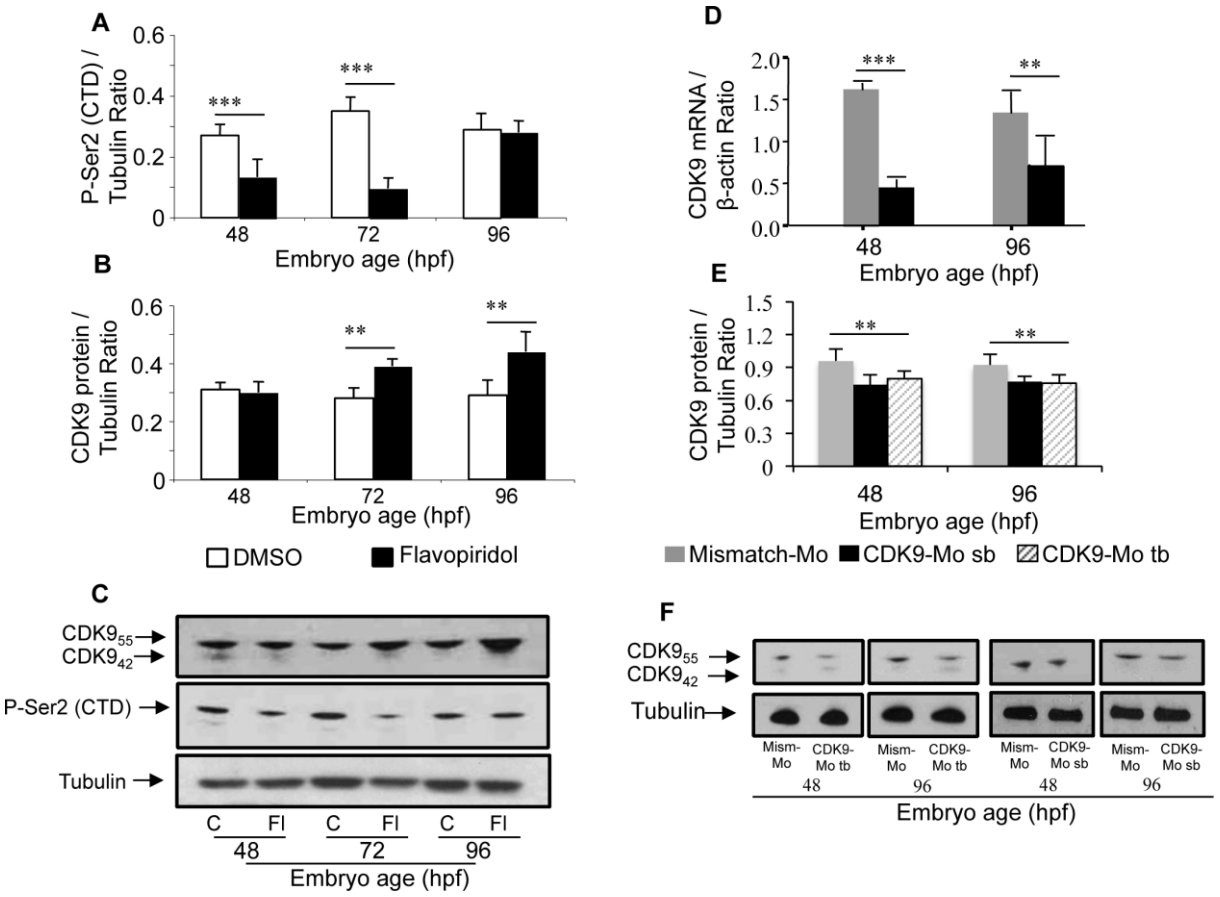

Figure 2– Effect of CDK9 inhibition on CDK9 level and its RNA-Pol II phosphorylation site (P-Ser2-CTD).

CDK9 mRNA (**A**) and protein (**B**) level were significantly reduced at 48 and 96 hpf following injection of CDK9-Mo (splice blocking (SB) and translation blocking (TB)). Panel **C** shows Western blot membranes showing CDK9 isoform-55 KDa which is dominant on the smaller isoform-42KDa. Effects of flavopiridol (panels **D,E,F**) on CDK9 protein expression at 48, 72 and 96 hpf and downstream effect on phosphorylation of P-Ser2-CTD. β -actin mRNA was used to normalize mRNA level, while tubulin was used to normalize protein level. (N=3 experiments, >10 embryos per group, **=p<0.01, ***=p<0.001, one-way ANOVA test followed by Bonferroni's post hoc test). Key - Fl - flavopiridol, C- control, Mism–Mo - Mismatch morpholino, CDK9-Mo-SB – CDK9 morpholino splice blocking, CDK9-Mo-TB - CDK9 morpholino translation blocking.

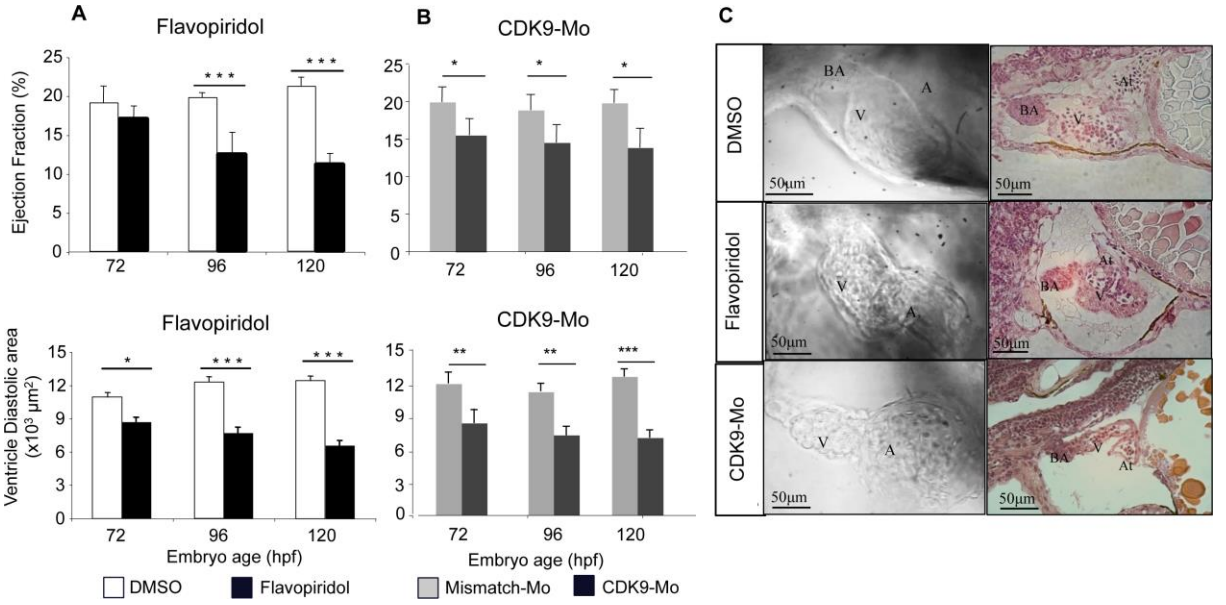

Figure 3 - Effects of CDK9 inhibition/knockdown on structure and function of the developing zebrafish heart.

For pharmacological inhibition (**A**), embryos were continuously exposed to vehicle (1% DMSO, clear bars) or flavopiridol (3umol/L, dark bars) from 24 to 120 hpf. For morpholino knockdown (**B**), embryo eggs 1-2 cell stage were injected with mismatch morpholino (clear bars) or CDK9 morpholino (black bars). Ventricle ejection fraction (**A,B,** upper panel) and diastolic area (**A,B**, lower panel) were assessed sequentially in the same embryos at 72, 96 and 120 hpf. Images in **C** show embryonic hearts following CDK9 modulation. (N=3 experiments, >10 embryos per experiment, *=p<0.05, **=p<0.01, ***=p<0.001. Two-way ANOVA test for repeated measures followed by Bonferroni's post-hoc test).

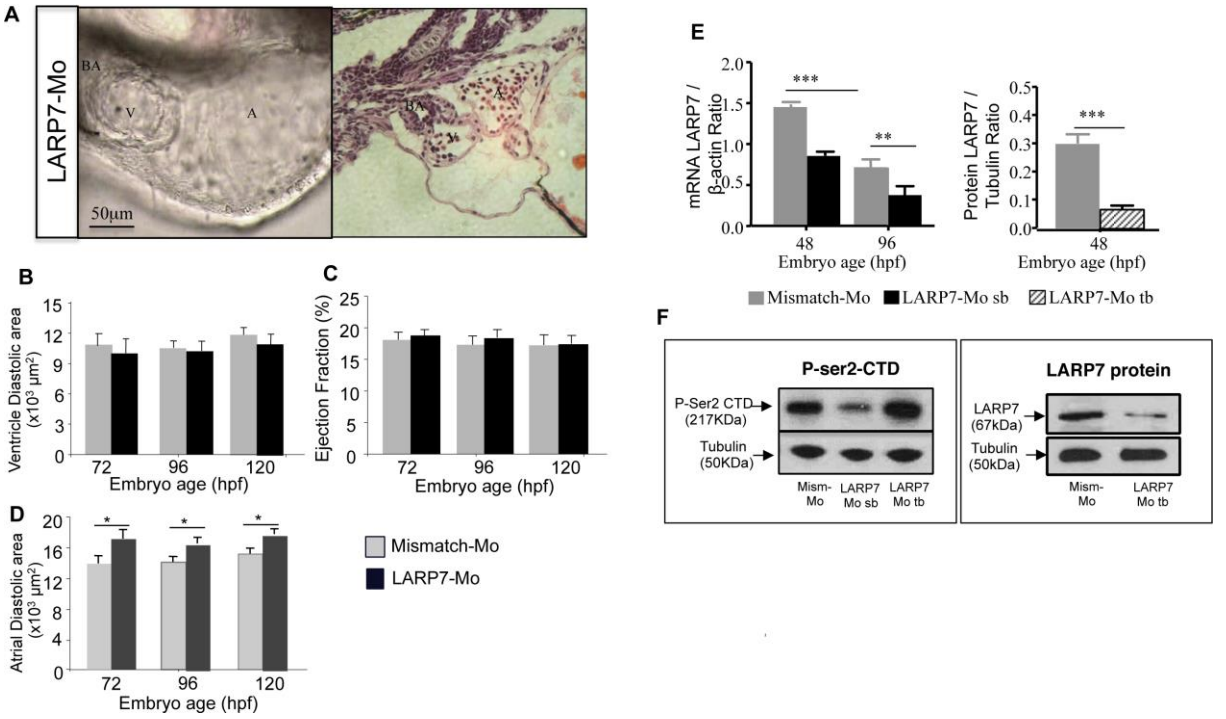

Figure 4 - Effects of LARP7 knockdown on cardiac structure and function.

A. LARP7 morpholino (splice blocking (SB) and translation blocking (TB)) resulted in normal heart development, here shown *in vivo* (left hand panel) and following H&E staining (right hand panel). Ventricular diastolic area (**B**) and ejection fraction (**C**) in LARP7 KD embryos was similar to controls (mismatch morpholino). A mild dilatation of the atrium (**D**) was observed in LARP7 KD embryos. LARP7 mRNA (**E**) and protein (**F**) were significantly reduced at 48 and 96 hpf. LARP7 morpholino-TB treatment caused increased phosphorylation of P-Ser2-CTD suggesting upregulation of CDK9 activity, (N=3 experiments, *=p<0.05, **=p<0.01, ***=p<0.001, two-way ANOVA followed by Bonferroni's post-hoc test).

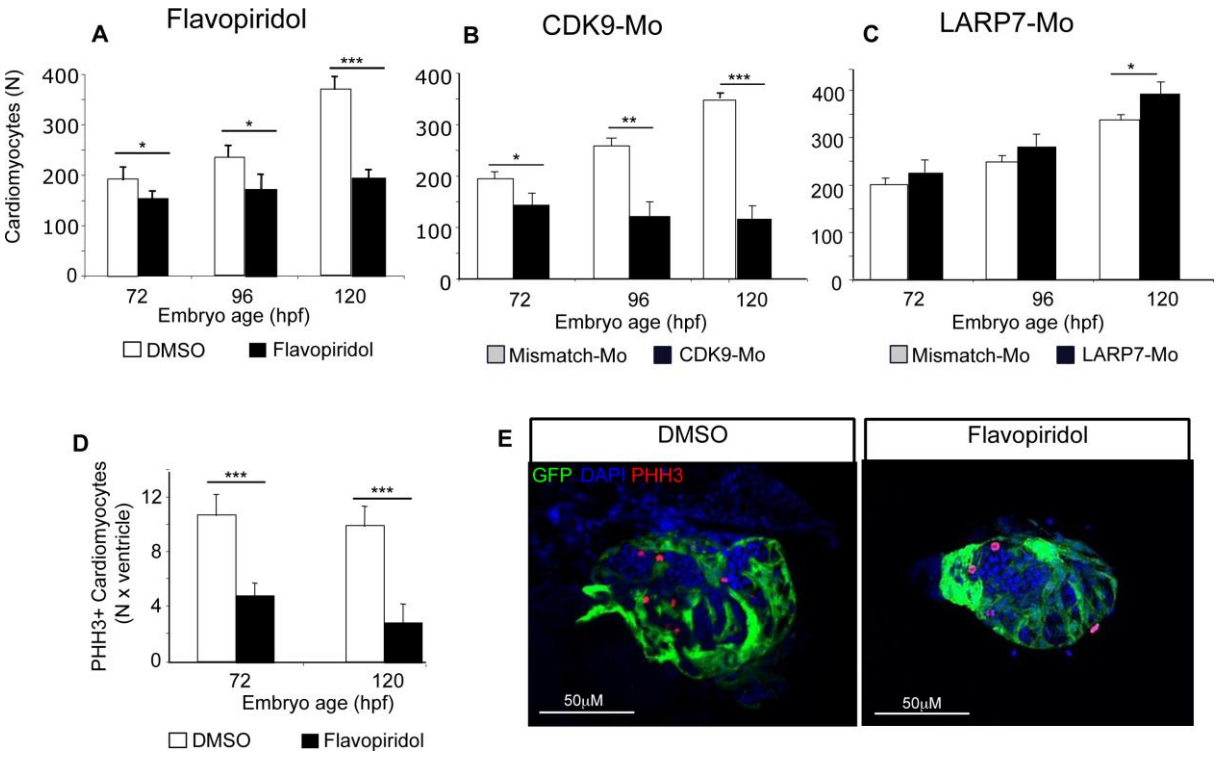

Figure 5 - Effects of CDK9 modulation on ventricle cardiomyocyte proliferation during early development of the zebrafish heart.

Effects of flavopiridol (**A**, clear bars – controls, black bars – flavopiridol 3umol/L) on total number of cardiomyocytes in the isolated embryonic zebrafish ventricle. Effects of CDK9 morpholino (**B**) and LARP7 morpholino (**C**) on total cardiomyocyte number in the embryonic ventricle (open bars- mismatch morpholino (controls), dark bars- splice blocking morpholino. Effects of flavopiridol on number of proliferating cardiomyocytes (**E**, open bars – controls, black bars – flavopiridol 3umol/L). Representative confocal images (**D**) of isolated embryonic *myl7*:GFP hearts stained with DAPI (blue) and phosphohistone H3 (PHH3, red nuclei) marking proliferating cardiomyocytes. Data are mean±sem, N=3 experiments, n=5 hearts per group,, *=p<0.05, **=p<0.01 ***=p<0.001, two-way ANOVA test.

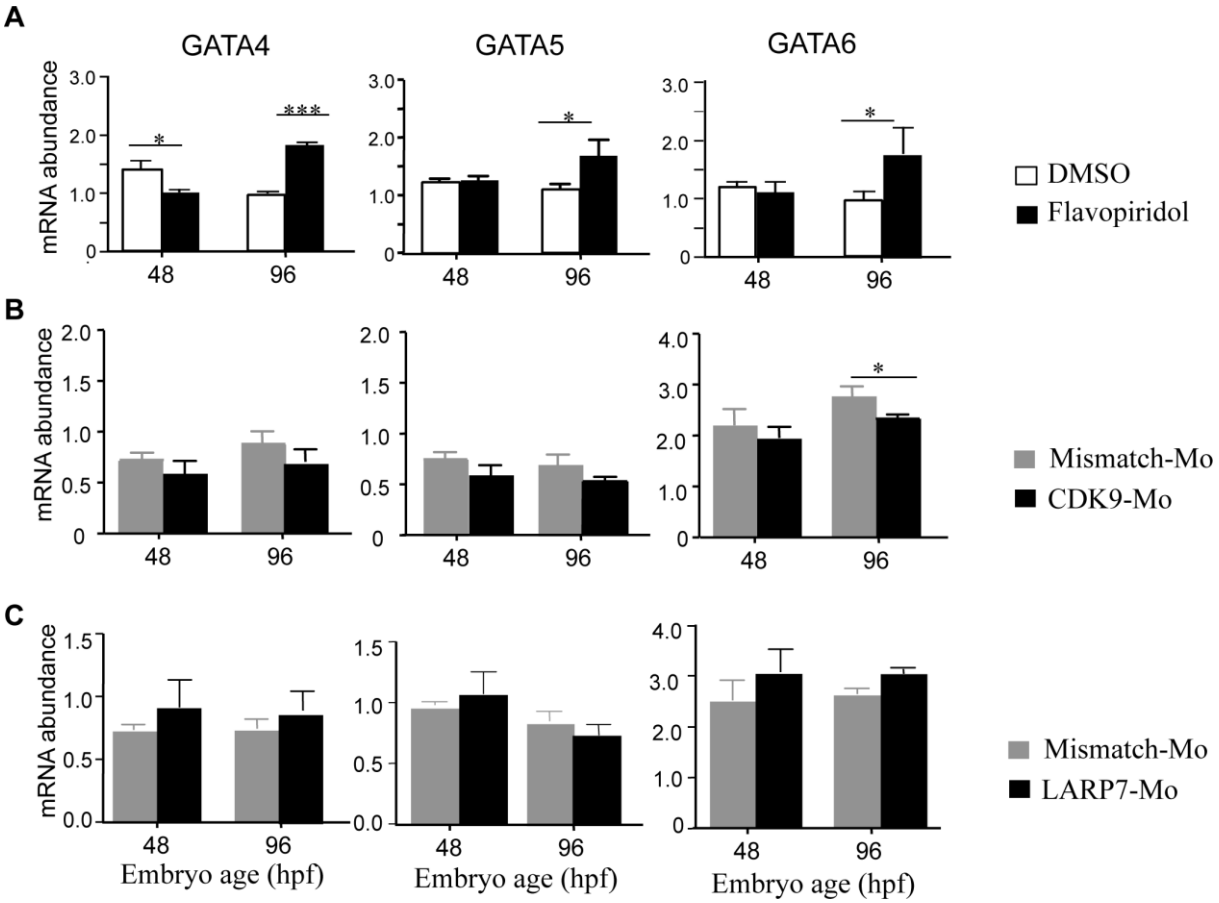

Figure 6 – Pattern of expression of GATA family genes in whole embryos at 48 and 96 hpf after flavopiridol or morpholino knockdown.

For pharmacological inhibition (**A**), embryos were continuously exposed to vehicle (1% DMSO, clear bars) or flavopiridol (3umol/L, dark bars) from 24 to 120 hpf. For CDK9 (**B**) or LARP7 (**C**) morpholino knockdown, embryo eggs 1-2 cell stage were injected with mismatch morpholino (clear bars) or gene targeting morpholino (black bars). mRNA was extracted from whole embryos (at least 10 embryos per group) at 48 and 96 hpf. Relative abundance of mRNA for GATA4, 5 and 6 was assessed by Q-PCR analysis. mRNA levels were normalised to β -actin in each case. N=3 experiments, *=$p<0.05$, ***=$p<0.001$, two-way ANOVA followed by Bonferroni's post-hoc test.

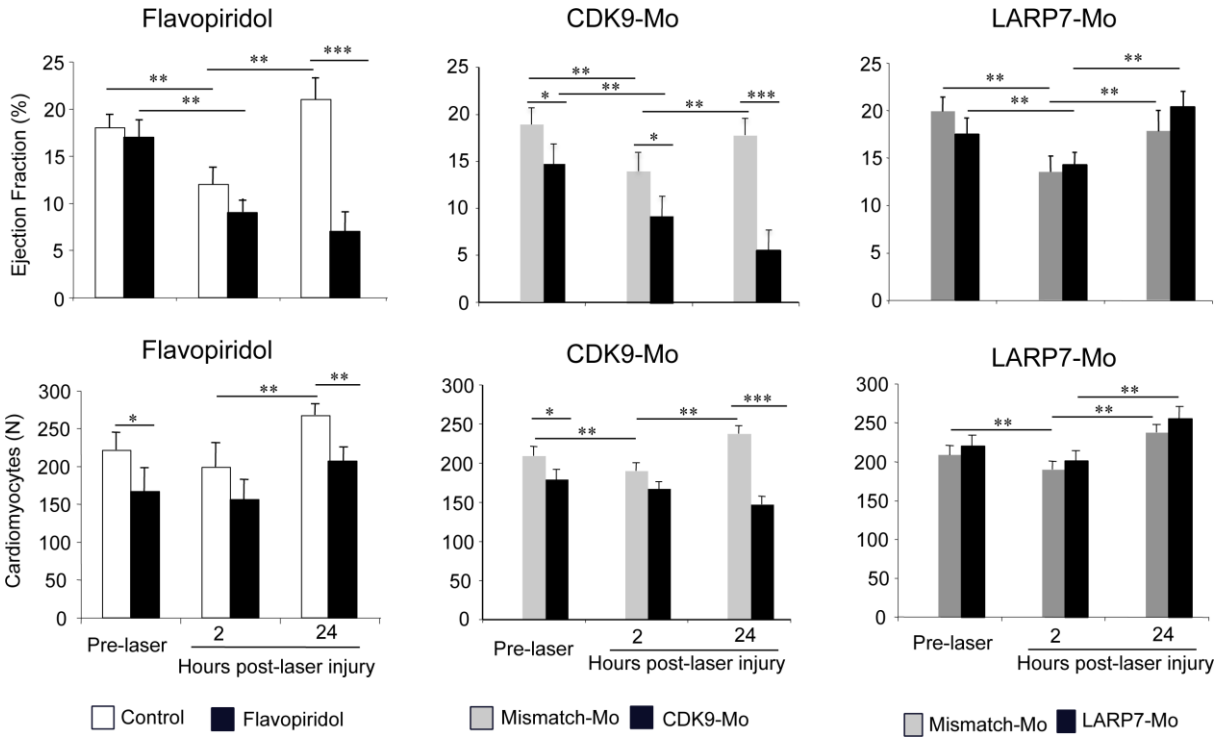

Figure 7 - Effects of CDK9 modulation on the response of the ventricle to laser injury. CDK9 activity was modulated pharmacologically and genetically by incubation in flavopiridol 3μ mol/L or injection of CDK9 morpholino and LARP7 morpholino (mismatch controls-grey bars, CDK9- or LARP7-Mo - dark bars) prior to injury. Laser injury (single pulse to the mid-ventricular cavity) was performed at 72 hpf. Ejection fraction and cardiomyocyte number were assessed pre-laser, 2 and 24 h post-laser injury, (N=3 experiments, n>10 embryos per experiment, two-way ANOVA test followed by Bonferroni's post-hoc test; *=$p<0.05$, **=$p<0.01$, ***=$p<0.001$).

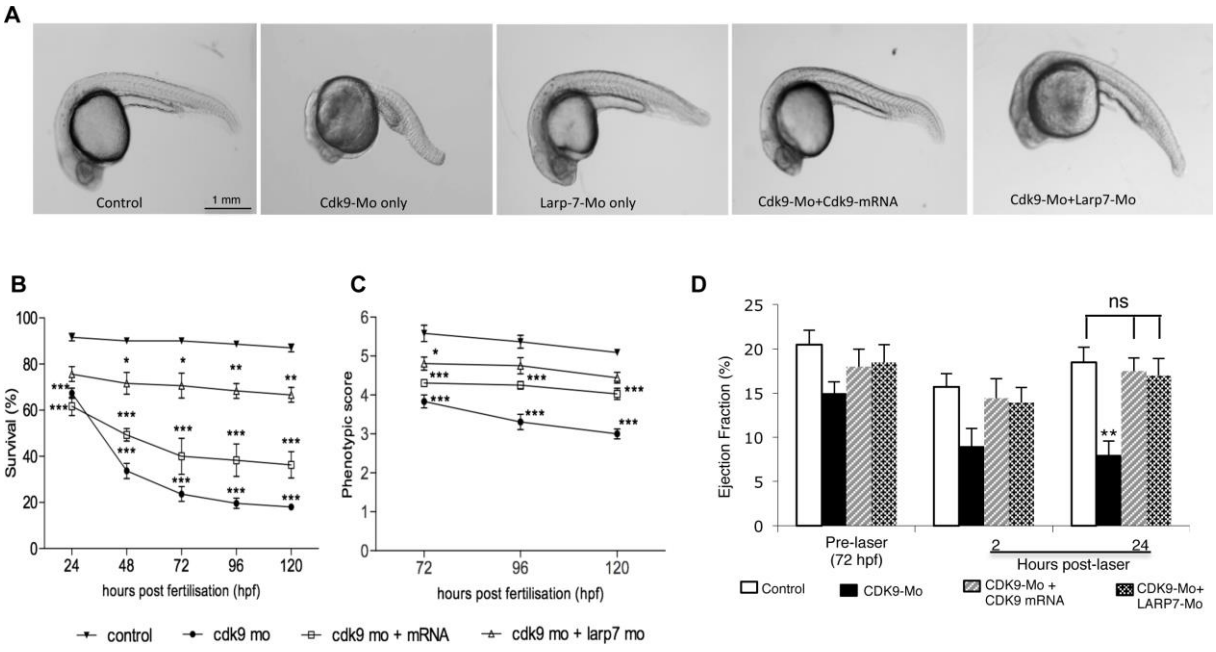

Figure 8 - Rescue CDK9-Mo using capped CDK9 mRNA or LARP7-Mo-SB.

Panel **A,B,C**. Survival and phenotype score in embryos treated with CDK9-Mo-SB, LARP7-Mo-SB, CDK9 + CDK9-mRNA, CDK9-Mo-SB + LARP7-Mo-SB assessed independently during first 120 hpf (N=3 experiments, n>50 embryos per group). Panel **D** – Effects of CDK9-Mo rescue (CDK9-RNA or LARP7-Mo-SB) on recovery of the cardiac function after laser injury (N=3, n=20-30 embryos per experiment). 2-way ANOVA and Bonferroni post hoc test, ns= non-significant, *p<0.05, **p<0.01 and ***p<0.001).